Drag Reduction on a Patterned Superhydrophobic Surface

Richard Truesdell,[1] Andrea Mammoli,[1] Peter Vorobieff,[1] Frank van Swol,[1,2] and C. Jeffrey Brinker[1,2]

[1]*Department of Mechanical Engineering, The University of New Mexico, Albuquerque, New Mexico 87131, USA*

[2]*Sandia National Laboratories, Albuquerque, New Mexico 87185, USA*

(Received 3 May 2006; published 26 July 2006)

We present an experimental study of a low-Reynolds number shear flow between two surfaces, one of which has a regular grooved texture augmented with a superhydrophobic coating. The combination reduces the effective fluid-surface contact area, thereby appreciably decreasing the drag on the surface and effectively changing the *macroscopic* boundary condition on the surface from no slip to limited slip. We measure the force on the surface and the velocity field in the immediate vicinity on the surface (and thus the wall shear) simultaneously. The latter facilitates a direct assessment of the effective slip length associated with the drag reduction.

DOI: 10.1103/PhysRevLett.97.044504 PACS numbers: 47.45.Gx, 47.61.−k, 47.85.lb

On the boundary between a viscous fluid and a solid surface the fluid velocity with respect to the surface is generally assumed to be zero (no-slip condition), and the amount of experience verifying this assumption is massive. From molecular dynamics considerations, while slip may occur on the boundary, its effects should be confined to the nanoscale realm. This notion is also well supported by experimental results [1,2]. Thus it is inevitable that in any fluid flow, one has to deal with shear caused by the difference between the free-stream velocity and the zero boundary velocity. This shear is the reason for the drag force on any body moving through fluid and for the pressure drop in any internal flow. The practical motivation to reduce the drag and the pressure drop is great, but is there anything that *can* be done?

In turbulent flows, a large fraction of the drag is produced by intermittent coherent structures. The energy dissipation by these structures can be reduced [3,4] by smoothing (laminarizing) the flow field. The next question that arises is if the *laminar* drag can be decreased without changing the macroscopic flow parameters (free-stream fluid properties, body size, geometry and surface temperature, etc.). Recent works [5–7] report evidence of such drag decrease obtained by reducing the effective contact area between the solid and the fluid. The fundamental importance of such flows over soft or patterned surfaces has been recently emphasized [8].

The contact area minimization was made possible by the development of superhydrophobic (SH) coatings. These coatings greatly decrease the energy of the interaction between the surface and the fluid, leading to unusually high contact angles for drops resting on SH surfaces [9]. If the solid surface is textured, with a regular or irregular pattern, a regime may emerge where there is insufficient energy to deform the fluid interface to bring it in contact with the entire solid surface [Cassie regime [9]], resulting in voids forming in the recessed parts of the pattern. For the parts of the fluid interface above the voids, the no-slip boundary condition will be no longer applicable, and the simplest boundary-condition assumption for these parts will be free slip (no shear on the interface), although in reality there still may be some small drag transmitted to the no-contact patches by the gas filling the voids. For a regular pattern of recessed grooves (free-slip) and protruding lands (no-slip), both analytical [10] and numerical [7,10] solutions show the drag to decrease with the characteristic size of the recessed surface features. As the feature size becomes larger, however, the fluid once again will come into contact with the recessed parts of the pattern, thus limiting the scale range of surface features that result in sliplike behavior.

While the feature sizes characteristic of the SH coating itself are usually on a submicron scale, voids can be greatly increased in size if the SH coating is applied to a textured surface [6,7] with features on the scale from microns to tens of microns, thereby producing a measurable change in the pressure drop [6] in an internal flow, in the terminal velocity of a drop rolling down the surface [7], or in the drag coefficient in an external flow [7]. It has been stipulated that, while there is no slip on the microscopic scale, the *macroscopic* boundary condition for the tangential velocity component u near a textured SH surface can be interpreted as Navier slip [11], with the slip velocity at the wall u_s proportional to the shear: $u_s = b(\partial u/\partial y)$. The direction y is normal to the wall, and the dimensional coefficient b is the *slip length*.

In this Letter, we present flow measurements near a regularly textured SH surface in shear flow showing *macroscopic* effective [12] [or apparent [8,12]] slip leading to drag reduction on the order of 20%. Moreover, the observed results cannot be entirely explained by the reduction of drag due solely to the formation of slip areas above the grooves in the pattern, suggesting that additional dynamic effects [e.g., related to nanobubble formation [13]] may play a role, as discussed below. In our experiment, reliable optical measurements are taken simultaneously with torque measurements. With the former, we measure the velocity field and extract the liquid-solid interface stress. The latter provide a direct measurement of the stress. Knowing the difference between the actual measured stress

and the stress inferred from the actual viscosity and the velocity profile assuming no-slip conditions, we can calculate the effective wall slip.

The experimental apparatus is a Couette cell designed for particle image velocimetry (PIV) measurements, Fig. 1. It is attached to a strain-controlled Rheometrics RFS8400 rheometer. A polymethyl methacrylate (PMMA) outside cylinder rotates at a carefully controlled rate, while a stationary inner cylinder is connected to the instrument's torque transducer. The immersed part of the inner cylinder terminates with a sharp edge. The volume contained within the walls of the inner cylinder is filled with air, virtually eliminating torque not due to the stress on the outward-facing surface of the inner cylinder. A flexible strip of polydimethylsiloxane (PDMS) with various combinations of patterning and SH coating is attached to this surface [Fig. 1(a), "stationary cylinder"]. A Newtonian fluid with the refractive index matching that of PMMA fills the gap between the inner cylinder and the outer cylinder. It is

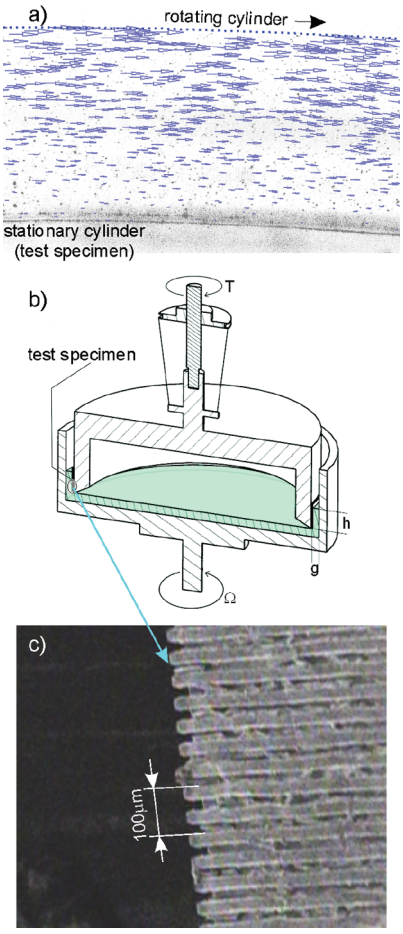

FIG. 1 (color). (a) Cross section of annular fluid region between inner and outer cylinders showing velocity vectors resolved by particle tracking. (b) Schematic of Couette apparatus. The outer cylinder rotates at a rate Ω; the inner cylinder is attached to the torque transducer. Shearing occurs in an annular region of fluid of width g and height h. (c) SEM image of SH-coated, grooved PDMS surface.

seeded with a small volume fraction (less than 10^{-5} by volume) of highly reflective TiO_2 particles with a characteristic size 200 nm. A pulsed Nd-YAG laser sheet illuminates a 200 μm thick planar section of the annular flow normal to the cylinder axis. A 2048×2048 16-bit digital camera records the particle image pairs. Unlike the earlier shear flow experiments [7], the surface patterning is deliberate [Fig. 1(c)], rather than a consequence of the breakup of the coating, and the fluid viscosity is much lower. The patterned SH surfaces are prepared as follows. First, we produce a high-resolution (± 2 μm) chrome-on-glass mask from a computer aided drafting drawing of the desired pattern. Then we apply this mask to a silicon wafer which has been precoated with negative photoresist. A 365 nm uv light exposes the assembly, hardening the photoresist under the clear areas of the mask. The unexposed photoresist is dissolved. With the resulting mold, we produce the PDMS substrates which are subsequently precoated with a thin gold layer, followed by dip-coating in aerogel solution of the SH material. The strips are applied to the stationary cylinder using double-sided adhesive tape. Here we present data acquired with a 25-μm pattern of alternating grooves and lands oriented streamwise [Fig. 1(c)]. At a series of strain rates ($1/s$, corresponding to the Reynolds number $\mathrm{Re} = 1.5$, to $50/s$, corresponding to $\mathrm{Re} = 75$), we measured the torque (3 clockwise, 3 counterclockwise readings to remove any bias on the torque transducer) and simultaneously acquired images for PIV diagnostics. We make accurate (± 10 μm) measurements of the gap dimension g and the height h of the working fluid by image analysis. As it is the outer cylinder that is spinning, secondary flows are not expected; however, centrifugal forces result in an increase of h with strain rate. The effect of this increase is removed during the normalization of the data. We record the output of the torque transducer to a National Instruments/Labview data acquisition workstation. Each torque measurement thus acquired averages 10 000 data points.

In the analysis of the PIV data, we are interested in the macroscopic effect of the surface treatment on the flow. We extract the slope of the linear approximation of the r-direction gradient of the measured velocity profile and compare it with one predicted theoretically and measured experimentally (smooth, uncoated surface) for the nonslip shear flow. The most marked reduction in gradient (up to 20%) is associated with the grooved-SH surface. The comparison of the velocity data for the uncoated-flat surface and the SH-grooved surface is shown in Fig. 2 ($\mathrm{Re} = 45$). For each case, we show about 10 000 velocity measurements obtained by adaptive particle tracking from four image pairs. The difference in velocity gradients is evident to the unaided eye. Furthermore, the velocity profiles provide insight in the slip mechanism. Near the outer surface, the velocity for the two cases is identical, about 13 cm/s. Near the inner surface, the velocity for the uncoated-flat surface is zero, while the velocity for the SH-grooved surface is 2–3 cm/s. In addition, the minimum velocity near the surface appears to curve downwards, while the

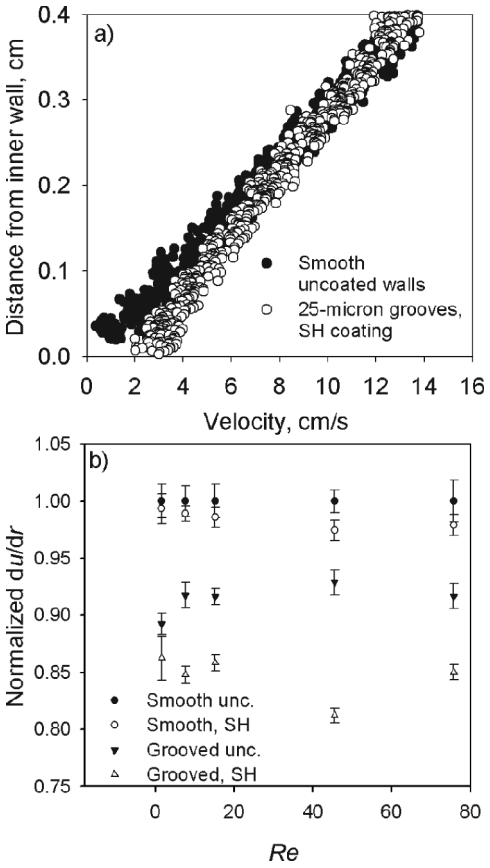

FIG. 2. (a) Velocity profiles for flat-uncoated surface and grooved-coated surface, Re = 45. (b) Decrease in the slope of the velocity profiles for various surface treatment-patterning combinations as a function of the Reynolds number. All slopes normalized by du/dr for smooth uncoated surface.

scatter in the data is increased. This is due to the finite thickness of the laser sheet enclosing about eight areas with zero slip (the lands) and eight regions of slip (the grooves). Near the boundary, velocity vectors represent particles traveling above slip and no-slip areas. On the other hand, there is no obvious difference between the velocity profiles with flat-uncoated surface or the flat-SH surface. The flat-SH surface is not perfectly smooth, with the surface features due to the SH coating alone being on submicron scale, which could account for some amount of effective slip. It is noteworthy that the grooved-uncoated surface profile shows more prominent effective slip than the smooth-coated surface, likely due to the fact that even the uncoated PDMS is hydrophobic (contact angle about 100° versus 156° for coated PDMS), which could be sufficient for voids retained in the grooves. The shape of the velocity profiles is in good agreement with theoretical predictions [14].

The torque data and the measured value of h can be used to plot the apparent viscosity as a function of the strain rate. From the physical interpretation of previous results [6,7], we expect a constant apparent viscosity, consistent with a slip velocity given by the Navier equation with constant coefficient. The experimental data [Fig. 3(a)] confirm this assumption. In addition, we observe a reduction in apparent viscosity in the SH-grooved experiment of over 20% with respect to the uncoated-flat sample experiment, in agreement with the PIV measurement. After correcting for the effect of the convex meniscus, the coated-flat surface results in a very small torque reduction, within experimental error from the uncoated-flat surface. Conversely, the uncoated-grooved experiments showed a 7%–8% reduction in apparent viscosity with respect to the reference surface. It appears that surface patterning applied even to the moderately hydrophobic PDMS surface (contact angle 100°) can result in some drag reduction due to formation of voids. In Fig. 3(b) we show effective slip lengths obtained from torque measurements as a function of strain rate. Two features are immediately obvious: first, the slip length is approximately a factor of 10 greater than the groove size, a larger than expected effect [similarly, slip lengths on the order of tens of microns have been recently reported on surfaces with micron-sized features [15]]. Second, within experimental error, the slip length does not depend on stress. It is also evident that the PIV measurements of slopes correspond directly to the measurements of apparent viscosity in Fig. 3(a). Here by "slip" we refer to the phenomenon of "apparent" or "effective" slip described in the literature, manifested by large-scale behavior of the flow consistent with Navier-like slip, while there is no slip on the microscopic level in areas where the fluid is actually in contact with the surface.

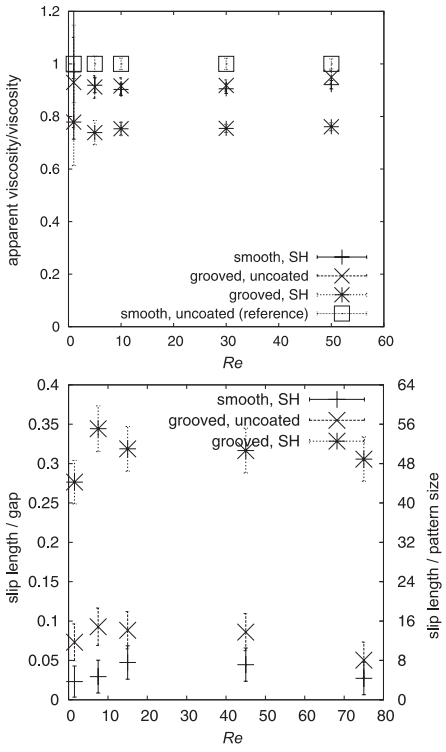

FIG. 3. (a) Apparent viscosity as a function of strain rate, and (b) slip length as a function of strain rate.

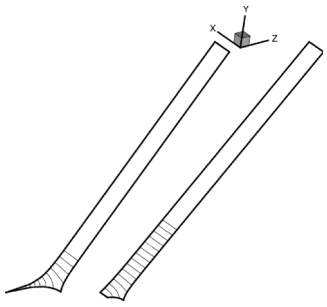

FIG. 4. Maps of tangential velocity (z axis in figure) in a Couette flow, obtained by FEM, for SH-grooved surface with contact area fraction of 0% (knife-edge, left) and 50% (experiments in this Letter, right). Direction normal to the grooves corresponds to the x axis. Note the difference in the slope of the velocity away from the SH surface, and the spread in velocity in the vicinity of the surface. The contour lines represent velocity values from 0 to 3, while the velocity of the top surface is 10. The ratio of feature size to gap in data shown here is 0.1 (0.0125 in the experiment).

Continuum mechanics cannot completely account for the large effective slip length we and others [15] observe. We performed a finite-element method (FEM) simulation (Fig. 4) to determine whether the combination of slip-stick boundary conditions at the grooved surface could reproduce slip lengths of the magnitudes we observe. In the FEM simulation, the ratio of feature size to flow dimension is 0.1, considerably larger than the ratio in the experiment of 0.0125. With the contact area fraction of 0.5 (same as elevated area to total surface area in experiment), the effective slip velocity that results is on the order of 5% of the velocity of the driving surface, while in the most favorable case of line contact, the slip velocity becomes 20% of the maximum velocity. For the case of the 0.0125 feature-gap ratio, the slip velocity in the latter most favorable case would be on the order of 0.5% of the maximum velocity, a factor of 40 smaller than what is observed experimentally. Thus, we conclude that additional mechanisms are responsible for the massive slip observed. Molecular dynamics simulations show that SH surfaces promote coexistence of both vapor and liquid phases near the surface. The formation of vapor also appears to be facilitated by shear stress [16]. Our experiments show that both the SH coating and the presence of longitudinal grooves are necessary to produce the macroscopic effective slip lengths. Thus it is likely that this combination produces additional mechanisms of drag reduction. The longitudinal grooves may provide a reservoir for the gas phase (fluid vapor or air). The network of cracks at the elevated parts of the pattern nominally in contact with the fluid would then form a pathway for an augmented vapor layer to be entrained between the fluid and the surface. Finally, the shear stress at the fluid interface would entrain the vapor, the availability of which is enhanced by the aforementioned mechanisms. In addition, recent studies also show possible slip on the fluid-fluid interface [8,17] (in our case, it would be between the entrained gas-vapor layer and the fluid above), which may also enhance the overall apparent slip. Other factors that could possibly contribute to the ''complex behavior at a liquid-solid interface'' [12] include pressure, surface charge, curvature, and impurities.

In the historical context, it is interesting that modern developments in materials science made possible the creation of patterned SH surfaces producing dramatic changes in the macroscopic fluid behavior near a solid boundary—yet this behavior is consistent with the theoretical considerations of Navier [11] dating back to the 1820s. While we conclude that the drag reduction or effective slip mechanism [6,7] proposed by earlier researchers is plausible, further analysis is required to accurately predict the ratio of slip length to feature size. The relatively simple phenomenon of effective slip can radically change many practical applications, as soon as reliable and durable SH coatings can be produced. Moreover, while SH coatings maximize drag reduction, moderately hydrophobic coatings in conjunction with patterning can still result in an appreciable decrease of drag. Because of the nature of the effective slip mechanism, the present technique may not be suited to high-pressure applications, where the surface tension is not sufficient to prevent the fluid from entering the grooves and contacting their entire surface. A strong need remains for theoretical and molecular dynamics studies providing a better understanding of the exact nature of the physical mechanism of drag reduction observed in this and other experiments [8].

The authors gratefully acknowledge support of US DOE Basic Energy Sciences, AFOSR, and FLAD.

[1] J. Baudry and E. Charlaix, Langmuir **17**, 5232 (2001).
[2] C.-H. Choi, J. A. Westin, and K. S. Breuer, Phys. Fluids **15**, 2897 (2003).
[3] D. Bonn *et al.*, J. Phys. Condens. Matter **17**, S1195 (2005).
[4] J. Drappier *et al.*, Europhys. Lett. **74**, 362 (2006).
[5] K. Watanabe *et al.*, AIChE J. **49**, 1956 (2003).
[6] J. Ou, B. Perot, and J. P. Rothstein, Phys. Fluids **16**, 4635 (2004).
[7] S. Gogte *et al.*, Phys. Fluids **17**, 051701 (2005).
[8] C. Neto *et al.*, Rep. Prog. Phys. **68**, 2859 (2005).
[9] D. Qúeŕe, Rep. Prog. Phys. **68**, 2495 (2005).
[10] E. Lauga and H. Stone, J. Fluid Mech. **489**, 55 (2003).
[11] C. Navier, Memoires de l'Academie Royale des Sciences de l'Institut de France **6**, 389 (1823).
[12] E. Lauga, M. P. Brenner, and H. Stone, in *Handbook of Experimental Fluid Dynamics*, edited by J. Foss and A. Yarin (Springer, New York, 2005), Chap. 15.
[13] X. H. Zhang and H. Jun, Prog. Chem. **16**, 673 (2004).
[14] J. T. Jeong, Phys. Fluids **13**, 1884 (2001).
[15] C.-H. Choi and C.-J. Kim, Phys. Rev. Lett. **96**, 066001 (2006).
[16] P. G. deGennes, Langmuir **18**, 3413 (2002).
[17] J. Koplik and J. R. Banavar, Phys. Rev. Lett. **96**, 044505 (2006).